Raman Spectroscopic Characterization of the Morphology of Polyethylene Reactor Powder

Li Hui Wang,† Roger S. Porter,* Howard D. Stidham, and Shaw L. Hsu

Departments of Polymer Science and Engineering and Chemistry, University of Massachusetts, Amherst, Massachusetts 01003

Received February 26, 1991; Revised Manuscript Received May 6, 1991

ABSTRACT: The morphological features of ultrahigh molecular weight polyethylene reactor powder polymerized both in slurry and in the gas phase have been characterized by use of the Raman active longitudinal acoustic mode (LAM) and disordered LAM found in the extremely low frequency region. These observations have been correlated to other specific spectroscopic features sensitive to structural order or disorder observed at higher frequencies. The range of molecular weight of the samples studied is from 0.96 to 12.4 × 10^6. A three-phase model of semicrystalline polymer, i.e., the crystalline phase, a meltlike amorphous phase, and a disordered interphase is consistent with our interpretation of the integrated intensities of characteristic bands assignable to each phase. Data demonstrate that the drawability of polyethylene reactor powder in the solid state can be explained by the content of the interfacial disordered region. Only samples with a lower interfacial content can be drawn to a high ratio. We conclude that chain entanglements in the region between lamellae restrict the ability of the samples to deform.

Introduction

It has recently been recognized that highly drawn polyethylene exhibits tensile moduli and strengths close to the theoretical values calculated for a perfect polyethylene crystal.[1-5] This conclusion has been achieved by combining solid-state extrusion with tensile drawing.[1,2] Thus, under optimum drawing conditions, an exceedingly high degree of chain extension and orientation can be realized.[6-8] From the drawing behavior found for single-crystal mats of ultrahigh molecular weight (UHMW) polyethylene, it was found that drawability and draw efficiency depend significantly on the techniques employed,[6,7] the sample molecular weight,[9] and the initial morphology,[10,11] particularly the last parameter. For example, the achievable draw ratio after recrystallization was only 5; from single-crystal mats grown from the same polyethylene sample, a draw ratio as high as 240 was obtained.[10]

The deformation mechanism associated with uniaxial drawing of semicrystalline polymers has been studied by X-ray and infrared.[12-14] It is normally viewed that the initial crystals consist of stacks of parallel lamellae which undergo phase transformation and twinning of the crystal lattice until the deformed lamellae reach maximum compliance for fracture by micronecking. The micronecks transform each lamellae into microfibrils consisting of folded-chain blocks broken from the lamella principally by chain slip in the boundary layers between adjacent blocks. Deformation along the orientation direction is initially accommodated in interlamellar regions, which cavitate and form microfibers. Yet higher deformation causes additional breaking of blocks of shear deformation, leading to a fibrillar morphology containing oriented crystals from the crystallized amorphous material at high elongations, crystal blocks broken from lamellae, and crystallites from chains drawn out of lamellae.[13] One can conclude from the deformation mechanism that the process for high deformation is limited by interlamellar links. A three-phase model describing the morphology of semicrystalline polymers has been recently proposed.[15] In this model, chain entanglements are located at the interphase. The limitation of crystal deformation is therefore directly related to interphase structure. In a recent study, we found that the drawability of reactor powders strongly depends on the polymerization temperature and processing conditions of the polyethylene. These reactor powders were synthesized by slurry and gas-phase processes. Molecular weight is not the dominant factor for the determination of the ultimate draw ratio. In fact, the interphase regions between the crystal and the amorphous phase appear to control limits of drawability.[15]

Only a few techniques are available to verify this hypothesis establishing the influence of the interphase morphology. Among these, Raman spectroscopy appears suitable for this purpose. The low-frequency Raman-active longitudinal acoustical mode (LAM) can directly provide the crystallite core thickness and its length distribution from the first-order vibration.[16-24] The mode frequency, $\Delta\nu$ (in cm^{-1} unit), and length, L (in Å), of the ordered sequence undergoing the vibration are related by the equation

$$\Delta\nu = \frac{m}{2cL}\left(\frac{E}{\rho}\right)^{1/2} \quad (1)$$

where m is an odd number and is the order of the vibration, c is the speed of light, ρ is the density of the crystalline vibrating sequence, and E is Young's modulus of the crystal in the chain direction. The Young's modulus measured for polyethylene crystals is 290 GPa.[25,26] With well-established structural parameters, the LAM frequency–length relationship can be expressed in a simple form as

$$\Delta\nu = 2827/L \ (cm^{-1}) \quad (2)$$

Crystalline thickness, thickness distribution, and defects have been interpreted from the central frequency and shape of the LAM bands observed.[27]

In an earlier Raman study, Strobl and Hagedorn described semicrystalline polyethylene as a superposition of three components consisting of the expected orthorhombic crystalline phase, a meltlike amorphous phase, and a disordered, anisotropic phase where chains are stretched but lack lateral order.[28] This analysis demonstrated that fractions involved in the three phases can be derived directly from the integrated intensities of characteristic bands without need for an additional calibration. Analysis was based on the assumption that the integrated intensity of the symmetric CH_2 bending A_g vibration near 1416 cm^{-1} can be used to measure the relative amount of CH_2 units

† On leave from the Materials Science Department, Fudan University, Shanghai, China.

0024-9297/91/2224-5535$02.50/0

Table I
Physical Properties of Reactor Powders As Measured by Raman Spectra and Thermal Analysis

sample	$M_v \times 10^{-6}$	c (DSC), %	α_c (Raman), %	α_a, %	α_b, %	DR_{max}	I_{int}
S30-12	12.42	66.8	65	17	18	6	0.27
S30-2	2.86	65.2	70	19	11	15	0.17
G85-1	0.96	64.7	61	25	14	22	0.22
G30-2	1.93	62.4	61	20	19	7	0.32
S85-5	4.80	68.9	72	23	5	98	0.07
S85-1	0.96	67.8	69	21	10	90	0.15
H1900	3.96	78.9	74	15	11	104	0.14

(α_c) present in the crystalline phase. The relative amount of the liquidlike amorphous phase can be determined by deconvoluting the spectrum in the twisting region into a narrow band centered at 1295 cm^{-1} and a broader component having its maximum intensity at 1303 cm^{-1} (α_{a_t}) or from the integrated intensity at 1080 cm^{-1} (α_{a_s}). The relative amount of the interfacial region α_b is thus given by

$$\alpha_b = 1.0 - (\alpha_a + \alpha_c) \quad (3)$$

where α_a is the average of α_{a_t} and α_{a_s}. This model has been utilized for explanation of a wide variety of crystalline polymer properties.[29-31]

In a number of subsequent studies, Snyder reported the observation of a liquidlike component in semicrystalline polyethylene by studying low-frequency Raman spectra in a different frequency range near 200 cm^{-1}.[32-34] The low-frequency Raman spectra of n-alkanes in the melt or in solution are dominated by intense bands appearing between 300 and 200 cm^{-1}. The central frequency of this band is proportional to $1/n^2$, where n is the number of skeletal atoms in the chain. The shape and central frequency of this intense component depend on the conformational distribution of the chain. For long chains, its frequency approaches a limiting value near 200 cm^{-1}. The bandwidth is determined by the dispersion about the average conformation. This band is generally referred as the disordered LAM or D-LAM. The frequency-length relationship has been used to characterize the highly amorphous component in semicrystalline polyethylene.[33]

In this study, these Raman methods are used to analyze the morphology of UHMW polyethylene reactor powders. Special attention was devoted to the characterization of the interfacial region. The relationship between the drawability of UHMW polyethylene reactor powders and their morphology is addressed.

Experimental Section

Seven as-received ultrahigh molecular weight polyethylene reactor powders were used in this study. Among them, the PE 1900 was manufactured by Hercules Co. All others were received from Union Carbide. These characterizations have been documented.[6,8] From viscosity measurements, these polymers were determined to have average molecular weights ranging from 0.96 to 12.4 $\times 10^6$ (see Table I). For our Raman study, all as-received samples were compression molded into a plate 1-mm thick at 150 kg/cm^2. To preserve the initial morphology of the reactor powder, the temperature used was 110 °C, which is 30 °C below the melting peak measured by differential scanning calorimetry (DSC).

The sample melting point and heat of fusion were measured on a DSC-4 Perkin-Elmer differential scanning calorimeter with a heating rate of 10 °C/min. The instrument was calibrated with an indium standard. The degree of crystallinity was calculated by assigning 69.2 cal/g as the enthalpy of fusion of a perfect polyethylene crystal.[35] The drawability of polyethylene reactor powder was determined by the maximum draw ratio (DR_{max}) obtained by solid-state coextrusion followed by tensile drawing, as described elsewhere.[6,8]

Raman spectra were obtained at ambient temperatures using a microprocessor-controlled Jobin-Yvon U-1000 laser Raman spectrometer. Excitation is provided by 5145-Å radiation from a Spectra-Physics Model 165-8 argon ion laser. In most of the Raman experiments, to prevent change in the initial morphology of the samples studied, the effective power of the incident excitation radiation at the sample is a relatively low value of 100 mW. Resolution was maintained at 2 cm^{-1}. A scattering geometry of 90° was used throughout. For quantitative LAM and D-LAM spectra, the background scattering was subtracted as described elsewhere.[36]

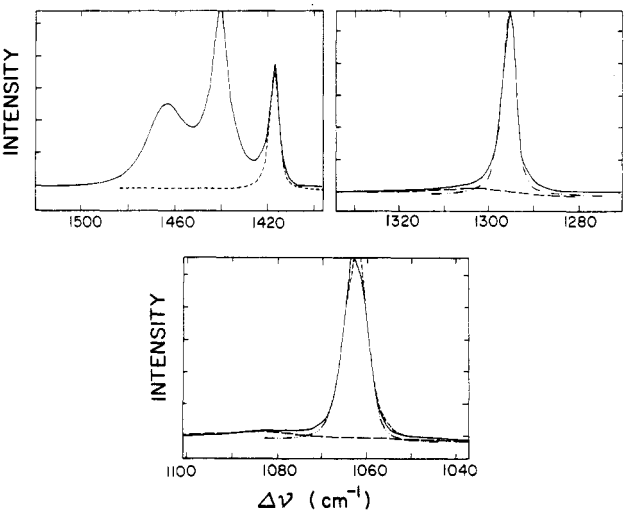

Figure 1. Typical types of Raman spectra indicating analysis. Deconvolution of the spectra observed in the CH_2 bending (1416 cm^{-1}), twisting (1303 and 1295 cm^{-1}), and skeletal stretching (1080 cm^{-1}) region by curve fitting.

Results and Discussion

In order to characterize the volume fraction of the various phases in polyethylene reactor powders, we have analyzed the integrated intensity of the Raman-active bands used in previous studies.[28,32,33] The integrated intensity of the twisting band is independent of chain conformation. Therefore, the sum of the intensities of the 1295- and 1303-cm^{-1} twisting bands is used as an internal intensity standard. The 1416-cm^{-1} CH_2 bending vibration is used to measure the relative amount of CH_2 units present in the crystalline phase. The amorphous content α_a is obtained from bands at 1080 and 1303 cm^{-1} independently. In all cases the integrated intensity was determined by deconvoluting the measured spectra, as shown in Figure 1. The percent of the chain units in the crystalline state α_c, in the liquid like state α_a, and in the interfacial state α_b, given by the Raman measurements, are shown in Table I together with the level of crystallinity obtained from the enthalpy of fusion, ΔH.

The crystallinity values, independently obtained with two different techniques, are in good agreement for nearly all samples studied (see Figure 2). The average percentage of amorphous content from the two different bands are given in the column labeled α_a. The content of the interfacial region is dependent on configurational regularity, molecular weight, and crystallization.[32,33] For example, the interfacial region is more significant for quenched samples than for those isothermally crystallized.[30] From Table I it can be seen that samples synthesized in a slurry at relatively higher temperatures

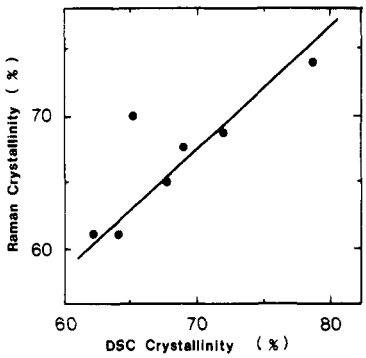

Figure 2. Relationship between the crystallinities measured by DSC and by Raman spectroscopy.

(85 °C for S85-5 and S85-1) have a higher degree of crystallinity. Samples obtained by gas-phase polymerization (G85-1 and G30-2, which were polymerized at 85 and 30 °C, respectively) have a lower degree of crystallinity. Both S85-1 and G85-1 were synthesized at 85 °C, but in different phases. The former has a higher crystallinity (69 ± 2%) than the latter (61 ± 2%). Moreover, interphase content is found to be a function of the polymerization condition. Higher interphase content is noted for polymers synthesized in the gas phase at 30 °C; the lowest interphase content is observed for samples polymerized at 85 °C in the slurry.

In order to clarify the factors governing drawability of polyethylene reactor powders, our interest centers on analysis of the interphase region. The interphase, as described by Strobl and Hagedorn, is a disordered phase of anisotropic nature located in a transition zone between crystalline and amorphous regions. From the mechanism of lamellae chain extension, it is known that the content of this phase is important for the drawing of semicrystalline polymers. The content of the interphase divided by the crystallinity of the measured sample is utilized as a measure of the level of disordered structure on the lamellae surface which should significantly influence deformation. This value is given in Table I in the column labeled I_{int}. Samples of lower I_{int} can be drawn to a higher draw ratio. Conversely, samples with a higher interfacial content can only be drawn to a limited value. Both S30-12 and G30-2, which can be drawn to ratios of approximately 6, have I_{int} values of approximately 0.3. This suggests that a large interfacial content located at the lamellae surface limits the initial deformation of the interfacial zone and prevents chain slippage at the boundary layers between adjacent lamellae upon extensive sample deformation.

The same conclusion can be obtained by analyzing the D-LAM observed in the 200–300-cm^{-1} region. As indicated by Snyder et al., the frequency and shape of D-LAM depends on the trans-to-gauche ratio and the average number of carbon atoms in the disordered sequences, which are essentially liquidlike.[32-34] Any substantial difference in the trans–gauche ratio would manifest in differences in the D-LAM band and its bandwidth, which increases with the number of gauche bonds. A representative low-frequency spectrum is shown in Figure 3. The prominent feature in the semicrystalline polyethylene is a broad D-LAM near 200 cm^{-1} and a band near 100 cm^{-1} characteristic of the orthorhombic crystalline phase. The integrated intensity of the D-LAM band is measured as before,[32-34] i.e., by using the sum of the intensities of 1295- and 1303-cm^{-1} bands as an internal standard, assumed to be independent of sample crystallinity. The combination of these two bands is referred to as the 1300-cm^{-1} band and the relative intensity of D-LAM is expressed as I_{200}/I_{1300}. The D-LAM was separated from the base line with

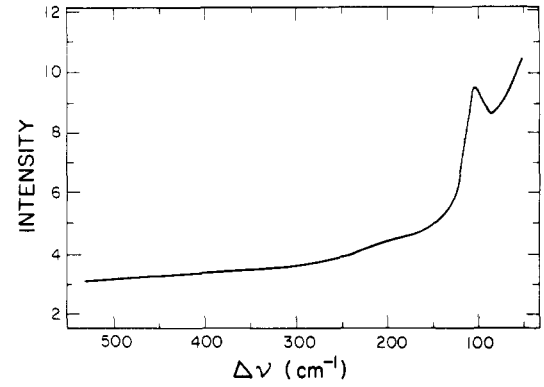

Figure 3. D-LAM band of sample S30-12.

Table II
Characteristic Interface Parameters of the PE Reactor Powder Measured from D-LAM Raman Spectra

sample	crystallizn condition	c (DSC), %	Δν (D-LAM)	$\Delta\nu_{1/2}$ (D-LAM)	I_{200}/I_{1300}
S30-12	powder	66.8	204	52.5	0.13
S30-2	powder	65.2			
G85-1	powder	64.7	197	60	0.16
G30-2	powder	62.4	207	54	0.11
S85-5	powder	68.9	197	41.5	0.087
S85-1	powder	67.8	207	48.5	0.086
H1900	powder	78.9	197	33.5	0.042
H1900	melt molded	42.7	203	40.5	0.17
S85-5	melt molded	56.2	194	49.5	0.23

the use of a computer by curve fitting. All data obtained are given in Table II. In our study, the D-LAM bands for all samples are located near 200 cm^{-1} (±4 cm^{-1}). This implies the absence of a substantial difference in the trans–gauche ratio for the samples studied. Due to the extremely broad bandshape, quantitative analysis is difficult. However, we have observed some differences in bandwidth, $\Delta\nu_{1/2}$. The S85-5, S85-1, and H1900 are three samples that are highly drawable and have a relatively narrower bandwidth and low band intensity. In comparison with others, a smaller number of gauche conformations exist in the interfacial region. These results are consistent with the measured values of the interfacial content as described above.

The H1900 reactor powder can be drawn to a draw ratio of 104 with a resultant modulus of 123 GPa.[15] The interphase content for this sample is the lowest found by D-LAM measurements, suggesting that more gauche bonds between lamellae imply more entangled chains in this region. From the deformation mechanism described above, it is anticipated that the initial deformation of crystalline regions will be difficult as the densely entangled interfacial region restricts the chain slip in the crystalline lamellae. It was indeed found for ductile polyethylene single crystals that the level of interfacial content is small.[31] Therefore, the highest drawability by coextrusion and post-drawing from polyethylene single-crystal mats would be expected.[2,6]

To understand the change of morphology after melting, reactor powder samples S85-5 and H1900 were compression molded at 180 °C for 10 min under identical pressures and then quenched in water. These samples were studied by Raman spectroscopy as described earlier. It was found that the band intensity at 200 cm^{-1} increased markedly and the bandwidth broadened (note the last two rows in Table II). Because the recrystallization proceeded in a highly viscous medium, from the melt with a more disordered layer formed at the lamellar surface where the molecular chains are extensively entangled, the crystallinity of these two melt-molded samples decreased sig-

Table III
Lamellar Thickness of UHMWPE Measured by LAM

sample	LAM band $\Delta\nu_{max}$, cm^{-1}	bandwidth $\Delta\nu_{1/2}$, cm^{-1}	lamellar thickness L, Å
S30-12	9.3	5.6	304
S30-2	10.2	6.0	284
G85-1	12.0	7.0	236
G30-2	8.9	5.2	319
S85-5	12.6	7.6	225
S85-1	12.5	7.8	227
H1900	10.7	5.5	263

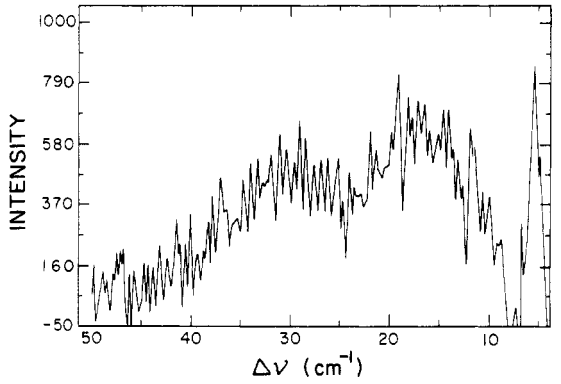

Figure 4. Deconvoluted LAM spectrum of the same sample as in Figure 5.

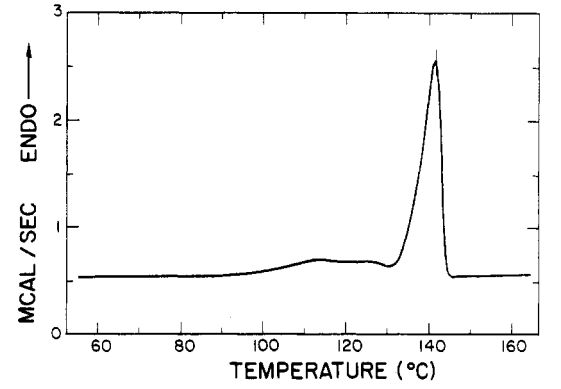

Figure 5. Thermogram of melt-molded sample S85-5 after annealing at 120 °C for 10 days.

nificantly. Accordingly, only low draw ratios can be readily attained from melt-crystallized UHMW polyethylene.[10,11]

The Raman data on lamellar microstructure are summarized in Table III. The lamellar thicknesses were calculated by using eq 2 without correction for temperature or frequency. All samples showed a lamellar thickness greater than the ones obtained for melt-crystallized samples. Nevertheless, this observation is not extremely useful as an explanation for the ability to draw polyethylene reactor powder. For the melt-crystallized samples, the LAM-1 band shifted to the high-frequency region. The melt-molded samples of S85-5 and H1900 were annealed at 120 °C in vacuo for 2 weeks. The degree of crystallinity obtained for these two samples is 56.4 and 55.5%, respectively, slightly higher than others. When these annealed samples were studied by Raman, it was found that two lamellae thicknesses represent two LAM peaks in the low-frequency region (see Figure 4). The corresponding thermogram of the same samples is shown in Figure 5. Multiple peaks are observed as well, due to the reorganization of crystals under the influence of heat. It is not possible, however, to conclude that these changes represent chain disentanglement at the interphase. Upon entanglement of long chain molecules, it appears difficult to disentangle by heat treatment below the melting point.

In conclusion, the morphological features of UHMW polyethylene reactor powders have been studied by Raman spectroscopy. Three-phase compositions of the polyethylene reactor powders have been derived from their characteristic bands. The crystallinity measured by Raman is in good agreement with the values obtained by DSC. The interfacial content of samples, measured by indirect deduction from both crystalline and amorphous content and D-LAM, exhibits a similar trend which may be used to correlate with the drawability of polyethylene reactor powders. A higher drawability can be correlated with a lower interfacial content.

Acknowledgment. We thank the Union Carbide Corp. for the polyethylene samples used in these studies and particularly for their syntheses by Dr. Burkhard E. Wagner. This research has been supported by the National Science Foundation, Polymers Program, Grant No. DMR-8919105.

References and Notes

(1) Kanamoto, T.; Porter, R. S. *Proc. Rolduc. Polym. Conf.*, 1988.
(2) Zachariades, A. E.; Kanamoto, T. *J. Appl. Polym. Sci.* **1988**, *35*, 1265.
(3) Sakurada, I.; Ito, T.; Nakamae, K. *J. Polym. Sci., Part C* **1966**, *15*, 75.
(4) Obser, G.; Blasenberg, S. *Colloid Polym. Sci.* 1970, *241*, 985.
(5) Matsuo, M.; Sawatari, C. *Macromolecules* **1986**, *19*, 2036.
(6) Kanamoto, T.; Tsuruta, A.; Tanaka, K.; Takeda, M.; Porter, R. S. *Polym. J.* **1983**, *15*, 327.
(7) Kanamoto, T.; Tsuruta, A.; Takeda, K.; Porter, R. S. *Macromolecules* **1988**, *21*, 470.
(8) Kanamoto, T.; Ohema, T., Tanaka, K. T.; Takeda, M.; Porter, R. S. *Polymer* **1987**, *28*, 1517.
(9) Kanamoto, T.; Porter, R. S. *Integration of Fundamental Polymer Science and Technology*: Lemstra, P. I., Elsevier, L. A., Eds.; Applied Science: London, 1989; Vol. 3, p 168.
(10) Zachariades, A. E.; Kanamoto, T. *Polym. Eng. Sci.* **1986**, *26*, 658.
(11) Smith, P., Chanzy, H. D.; Rotzinger, B. P. *Polym. Commun.* **1985**, *26*, 258.
(12) Peterlin, A. *J. Mater. Sci.* **1971**, *6*, 490.
(13) Adams, W. W.; Yang, D.; Thomas, E. L. *J. Mater. Sci.* **1986**, *21*, 2239.
(14) Brady, J. M.; Thomas, E. L. *Polymer* **1989**, *30*, 1615.
(15) Wang, L. H.; Ottani, S.; Porter, R. S. Submitted for publication.
(16) Schaufele, R. F.; Shimanouche, T. *J. Chem. Phys.* **1967**, *47*, 3605.
(17) Krimm, S.; Jakes, J. *Macromolecules* **1971**, *4*, 605.
(18) Peterlin, A.; Olf, H. G.; Peticolas, W. L.; Hibler, G. W.; Lippert, J. L. *J. Polym. Sci., Part B* **1971**, *9*, 583.
(19) Olf, H. G.; Peterlin, A.; Peticolas, W. L. *J. Polym. Sci., Polym. Phys. Ed.* **1974**, *12*, 359.
(20) Wang, Y. K.; Waldman, D. A.; Stein, R. S.; Hsu, S. L. *J. Appl. Phys.* **1982**, *53*, 659.
(21) Glotin, M.; Mandelkern, L. *J. Polym. Sci., Polym Phys. Ed.* **1983**, *21*, 29.
(22) Snyder, R. G.; Krause, S. J.; Scherer, J. R. *J. Polym. Sci., Polym. Phys. Ed.* **1978**, *16*, 1593.
(23) Snyder, R. G.; Scherer, J. R. *J. Polym. Sci., Polym. Phys. Ed.* **1980**, *18*, 421.
(24) Glotin, M.; Mandelkern, L. *J. Polym. Sci., Polym. Lett. Ed.* **1983**, *21*, 807.
(25) Koenig, J. L.; Tabb, D. L. *J. Macromol. Sci., Phys.* **1974**, *B9*, 141.
(26) Strobl, G. R.; Ecked, R. *J. Polym. Sci., Polym. Phys. Ed.* **1976**, *14*, 913.
(27) Reneker, D. H.; Fanconi, B. *J. Appl. Phys.* **1975**, *46*, 4144.
(28) Strobl, G. R.; Hagedorn, W. *J. Polym. Sci., Polym. Phys. Ed.* **1978**, *16*, 1181.
(29) Mandelkern, L. *Faraday Soc. Discuss.* **1979**, *68*, 310.
(30) Glotin, M.; Mandelkern, L. *Colloid Polym. Sci.* **1982**, *260*, 182.
(31) Glotin, M.; Domszy, R.; Mandelkern, L. *J. Polym. Sci., Polym. Phys. Ed.* **1983**, *21*, 285.
(32) Snyder, R. G.; Strauss, H. L. Elliger, C. A. *J. Phys. Chem.* **1982**, *86*, 5145.
(33) Snyder, R. G.; Schlotter, N. E.; Alamo, R.; Mandelkern, L. *Macromolecules* **1986**, *19*, 621.
(34) Snyder, R. G. *J. Chem. Phys.* **1982**, *76*, 3921.
(35) Magill, J. H. *J. Appl. Phys.* **1964**, *35*, 3249.
(36) Wang, L. H.; Ottani, S.; Porter, R. S. To be submitted for publication.

Registry No. Polyethylene (homopolymer), 9002-88-4.